

Intrinsic function of the peptidylarginine deiminase PADI4 is dispensable for normal haematopoiesis

Christine Young^{1,2}, John R. Russell¹, Louie N. Van De Lagemaat^{2,3},
Hannah Lawson^{2,3}, Christopher Mapperley^{2,3}, Kamil R. Kranc^{2,3,*} and
Maria A. Christophorou^{1,2,4*}

¹MRC Human Genetics Unit, The Institute of Genetics and Molecular Medicine, University of Edinburgh, Edinburgh EH4 2XU, United Kingdom

²Centre for Regenerative Medicine, University of Edinburgh, Edinburgh, United Kingdom

³Laboratory of Haematopoietic Stem Cell & Leukaemia Biology, Centre for Haemato-Oncology, Barts Cancer Institute, Queen Mary University of London, London EC1M 6BQ, United Kingdom

⁴Babraham Institute, Cambridge CB22 3AT, United Kingdom

*Correspondence to: Maria A. Christophorou (maria.christophorou@babraham.ac.uk) and Kamil R. Kranc (kamil.kranc@qmul.ac.uk). These authors contributed equally.

Keywords: peptidylarginine deiminase IV (PADI4), haematopoietic development, bone marrow, differentiation, regeneration, ageing.

Summary Statement

Inhibition of the pluripotency regulator peptidylarginine deiminase IV (PADI4) does not affect normal haematopoietic development or function, suggesting that targeting it as a therapy can be well tolerated.

Abstract

Peptidylarginine deiminases (PADIs) are strongly associated with the development of autoimmunity, neurodegeneration and cancer but their physiological roles are ill-defined. The nuclear deiminase PADI4 regulates pluripotency in the mammalian pre-implantation embryo but its function in tissue development is unknown. PADI4 is primarily expressed in the bone marrow, as part of a self-renewal-associated gene signature. It has been shown to regulate the proliferation of multipotent haematopoietic progenitors and proposed to impact on the differentiation of

haematopoietic stem cells (HSCs), suggesting that it controls haematopoietic development or regeneration. Using conditional *in vivo* models of steady state and acute *Padi4* ablation, we examined the role of PADI4 in the development and function of the haematopoietic system. We found that PADI4 loss does not significantly affect HSC self-renewal or differentiation potential upon injury or serial transplantation, nor does it lead to HSC exhaustion or premature ageing. Thus PADI4 is dispensable for cell-autonomous HSC maintenance, differentiation and haematopoietic regeneration. This work represents the first study of PADI4 in tissue development and indicates that pharmacological PADI4 inhibition is likely to be tolerated without adverse effects.

Introduction

Haematopoietic stem cells (HSCs) possess self-renewal capacity and multi-lineage differentiation potential, and are therefore able to replenish all blood cell lineages, sustaining normal and post-injury haematopoiesis. In addition to transcription factors, which directly facilitate or inhibit gene transcription, a central mechanism involved in stem cell fate decisions is the modulation of expression of stem cell and differentiation genes achieved *via* epigenetic mechanisms such as histone modifications. Indeed, several studies have shown that histone-modifying enzymes are essential for normal haematopoiesis (Chan *et al.*, 2003; Loizou *et al.*, 2009; Ou *et al.*, 2011; Thieme *et al.*, 2013; Wang, Peterson and Loring, 2014; Liu *et al.*, 2015; Greenblatt, Liu and Nimer, 2016).

Peptidylarginine deiminase (PADI, or PAD) enzymes catalyze citrullination, the post-translational conversion of protein arginine residues to the non-coded amino acid citrulline. The five PADI family members are structurally similar and likely to operate *via* common regulatory mechanisms (Arita *et al.*, 2004; Slade *et al.*, 2015), but they show varying tissue distributions and sub-cellular localisations, suggesting that they have specific organismal roles. PADI deregulation is strongly associated with disease development (Wang and Wang, 2013; Lewis and Nacht, 2016). Aberrantly high citrullination levels underlie the development of autoimmunity (rheumatoid arthritis, systemic lupus erythematosus and ulcerative colitis), and are strongly associated with the development neurodegeneration (multiple sclerosis) and cancer (Suzuki *et al.*, 2003; Musse *et al.*, 2008; Zhang *et al.*, 2011; Wang and Wang, 2013; Witalison *et al.*, 2015; Yuzhalin *et al.*, 2018). For this reason significant efforts have been devoted towards generating inhibitors against PADIs (Lewis and Nacht, 2016), necessitating a better understanding of their physiological functions.

The nuclear deiminase PADI4 citrullinates core and linker histones and has well-established roles in the regulation of gene transcription and chromatin compaction (Cuthbert *et al.*, 2004; Wang *et al.*, 2004; Tanikawa *et al.*, 2009, 2018; Guo and Fast, 2011; Zhang *et al.*, 2011; Stadler *et al.*, 2013; Wang and Wang, 2013; Christophorou *et al.*, 2014). We previously showed that PADI4 regulates the establishment of pluripotency during mammalian pre-implantation embryo development and cell reprogramming (Christophorou *et al.*, 2014), however it is not known whether PADI4 plays a role in tissue development. Out of all mammalian tissues, *Padi4* is most highly expressed in the bone marrow (BM) and peripheral blood (PB) and is one of the top 50 genes associated with self-renewal, as determined by the fact that it is expressed in HSCs, down-regulated upon differentiation to multi-lineage progenitors, but up-regulated in leukaemia stem cells (Krivtsov *et al.*, 2006). More recent studies showed that haematopoietic multipotent progenitor cells from constitutive *Padi4*-null mice exhibit increased proliferation (Nakashima *et al.*, 2013). Additional work showed that PADI4 regulates the expression of c-Myc and acts as a co-activator of translocated in leukaemia 1 (Tal1) (Nakashima *et al.*, 2013; Kolodziej *et al.*, 2014). c-Myc and Tal1 are critical transcriptional regulators in the haematopoietic system, suggesting that PADI4 regulates the differentiation of haematopoietic stem or progenitor cells (Kolodziej *et al.*, 2014). Taken together, these findings suggest that PADI4 functions in the regulation of haematopoiesis.

To understand the role of PADI4 in normal haematopoiesis, HSC maintenance, haematopoietic regeneration and ageing, we carried out a systematic analysis using mouse models of constitutive and inducible *Padi4* deletion from the haematopoietic system. We demonstrate that HSCs do not require intrinsic PADI4 to self-renew, sustain long-term multilineage haematopoiesis or respond to haematopoietic injury. Moreover, by investigating long-term consequences of *Padi4* deletion, we show that *Padi4* loss does not lead to HSC exhaustion or premature ageing.

Results

***Padi4* ablation does not significantly affect steady-state haematopoiesis**

Mammalian PADI enzymes exhibit tissue specific expression and PADI4 is expressed mainly the BM and in peripheral blood neutrophils, eosinophils and monocytes (Nakashima, Hagiwara and Yamada, 2002; Vossenaar *et al.*, 2004; Krivtsov *et al.*, 2006; Nakashima *et al.*, 2013). Global transcriptomic analyses of sorted BM cell populations shows that *Padi4* expression is expressed most highly in haematopoietic stem and progenitor cells (Figure 1A), while PADI4 protein is readily

detectable in the BM (Figure 1B). To determine the functional significance of PADI4 in steady-state haematopoiesis and HSC self-renewal, we deleted *Padi4* specifically from the haematopoietic system using the *Vav-iCre* system. *Vav-iCre* mice (de Boer *et al.*, 2003) constitutively express the codon-improved Cre (iCre) (Shimshek *et al.*, 2002) driven by the *Vav* regulatory elements (Ogilvy *et al.*, 1999), resulting in haematopoietic-specific gene deletion shortly after the emergence of definitive HSCs (Chen *et al.*, 2009) and ensuring recombination in all HSCs (Buza-Vidas *et al.*, 2011; Paris *et al.*, 2019). We bred these mice to *Padi4^{fl/fl}* mice (Hemmers *et al.*, 2011), in which *Padi4* exons 9 and 10 are flanked by *loxP* sites. These exons contain aspartate 352, which is part of the active site, as well as four additional residues (Q351, E353, E355, D371), which are essential for Ca²⁺ binding and activation of the enzyme (Arita *et al.*, 2004). The resulting *Padi4^{fl/fl};Vav-iCre* mice (referred to as *Padi4^{CKO}*, for *Padi4* conditional knock-out, hereafter) completely lack PADI4 protein expression in the BM (Figure 1B). These mice were compared to *Padi4^{fl/fl}* mice (referred to as *Padi4^{CTL}*, for *Padi4* control, hereafter) in all subsequent analyses. *Padi4^{CKO}* and *Padi4^{CTL}* mice showed normal Mendelian distribution, had comparable survival and did not display any obvious defects. To enumerate cells at different levels of the haematopoietic differentiation hierarchy, we next carried out immunophenotypic analyses of *Padi4^{CKO}* mice. In agreement with a previous report (Nakashima *et al.*, 2013), *Padi4^{CKO}* mice had increased numbers of Lin⁻Sca-1⁺c-Kit⁺ (LSK) cells but similar numbers of total white blood cells (WBC) and lineage restricted myeloid and erythroid of Lin⁻Sca-1⁻c-Kit⁺ (LK) progenitor cells compared to *Padi4^{CTL}* mice (Figure 1C). Further analysis of the LSK compartment showed normal numbers of LSKCD48⁻CD150⁺ HSCs, LSKCD48⁻CD150⁻ multipotent progenitors (MPPs), LKSCD48⁺CD150⁺ primitive haematopoietic progenitors (HPC-2) and an increase in LSKCD48⁺CD150⁻ haematopoietic progenitor cell-1 (HPC-1) population in *Padi4^{CKO}* mice compared to *Padi4^{CTL}* mice (Figure 1D). We observed an increase in common lymphoid progenitors (Lin⁻c-Kit^{lo}Sca^{lo}IL7R α ⁺ cells) in *Padi4^{CKO}* mice compared to *Padi4^{CTL}* mice (Figure 1E). However, the numbers of myeloid and erythroid progenitors, CD11b⁺Gr1⁻ and CD11b⁺Gr1⁺ differentiated myeloid cells, CD19⁺ B cells and Ter119⁺ erythroid cells in the BM were comparable between *Padi4^{CKO}* and *Padi4^{CTL}* mice (Figure 1F). These results were mirrored in *in vitro* colony forming cell (CFC) assays where there was no difference in colony counts between the two genotypes (Figure 1G). In addition, numbers of thymic T-cells were unaffected (Supplementary Figure 1A). PB analysis showed that the numbers of circulating blood cells and haemoglobin parameters were completely unaffected by *Padi4* deletion (Supplementary Figure 1B). Analysis of the spleens showed a modest increase in differentiated cells in *Padi4^{CKO}* mice with an overall increase in WBC

counts, indicating extramedullary haematopoiesis (Figure 1H). In conclusion, despite mild extramedullary haematopoiesis, *Padi4* deletion has no major impact on BM steady-state haematopoiesis.

***Padi4* is dispensable for HSC maintenance**

To assess the requirement for *Padi4* in HSC maintenance, we performed competitive HSC transplantation assays. CD45.2⁺LSKCD48⁻CD150⁺ HSCs sorted from *Padi4*^{CKO} and control (*Padi4*^{CTL}) mice were competitively transplanted into lethally irradiated wild-type syngeneic CD45.1⁺/CD45.2⁺ recipients (Figure 2A). Peripheral blood analysis showed no difference in CD45.2⁺ donor-derived chimerism in primary recipients of the *Padi4*^{CKO} HSCs when compared to recipients of *Padi4*^{CTL} HSCs (Supplementary Figure 2A). BM analysis at 16 weeks post transplantation showed that HSCs of both genotypes efficiently reconstituted long-term multi-lineage haematopoiesis, while donor-derived cells contributed equally to BM HSC and primitive cell compartments of the primary recipient mice (Figure 2B). No difference in CD45.2⁺ cell engraftment was found in the spleen of recipient mice and both *Padi4*^{CTL} and *Padi4*^{CKO} donor derived cells contributed equally to differentiated cell populations in the spleen (Figure 2C). Moreover, *Padi4*^{CKO} LSK cells sustained long-term BM reconstitution in secondary recipients comparably to *Padi4*^{CTL} LSK cells (Figure 2D), while equal engraftment of CD45.2⁺ cell engraftment was observed in spleen (Figure 2E) of the secondary recipients. In addition, no difference in CD45.2⁺ cell engraftment was found in PB (Supplementary Figure 2B). These experiments revealed that HSCs do not require *Padi4* to self-renew and sustain long-term multi-lineage haematopoiesis upon transplantation.

Acute Padi4 deletion does not affect haematopoietic development

Given that *Vav-iCre* recombines in the embryo soon after the emergence of definitive HSCs, it is possible that *Vav-iCre*-mediated *Padi4* deletion may activate compensatory mechanisms that bypass *Padi4* deficiency. To rule this out, we examined HSC maintenance following acute *Padi4* ablation. We generated *Padi4*^{fl/fl};*Mx1-Cre* mice (referred to as *Padi4*^{IKO}, for *Padi4* inducible knock-out, hereafter) in which efficient recombination in the BM is induced by treatment with Poly I:C (Kühn *et al.*, 1995) and leads to complete loss of PADI4 protein (Figure 3A). *Padi4*^{IKO} and *Padi4*^{CTL} mice received 6 injections of 300 µg Poly I:C, on every other day, and were culled and analysed 4 weeks following the final administration. We found that acute deletion of *Padi4* had no effect on any BM cell compartment analysed (Figure 3B). To test whether acute *Padi4* deletion affects post-transplantation haematopoietic reconstitution, we transplanted CD45.2⁺

unfractionated BM cells from *Padi4*^{CKO} or *Padi4*^{CTL} mice with support CD45.1⁺ BM cells to lethally irradiated recipient mice. Following efficient CD45.2⁺ cell engraftment (8 weeks post transplantation), the mice received 6 doses of Poly I:C resulting in efficient *Padi4* deletion in donor-derived CD45.2⁺ cells (Figure 3C). The contribution of CD45.2⁺ cells to the PB of the recipients was quantified at 4, 8, 12, 18 and 22 weeks post transplantation and no differences were observed (Supplementary Figure 3). The donor-derived contribution of CD45.2⁺ cells to BM cell compartments of the recipients, including total WBC, LSK, LK and HSCs of the recipients was similar regardless of the genotype of transplanted CD45.2⁺ cells, as was the CD45.2⁺ cell contribution to differentiated cell lineages in the BM (Figure 3D).

***Padi4* is dispensable for the regenerative capacity of HSCs**

To test the role of *Padi4* in HSC regenerative capacity upon haematopoietic injury, we treated adult (8-12 week) *Padi4*^{CKO} and *Padi4*^{CTL} mice with 5-fluorouracil (5-FU). Mice received 3 injections of 5-FU 10 days apart and BM was analysed 10 days following the final dose (Figure 4A). We observed no difference in numbers of HSCs, LSK, LK cell compartments or differentiated cells in the BM of *Padi4*^{CKO} mice compared to *Padi4*^{CTL} mice (Figure 4B and Supplementary Figure 4). Therefore, PADI4 is dispensable for the ability of HSCs to respond to haematopoietic stress.

***Padi4* ablation does not lead to HSC exhaustion upon ageing**

To investigate the long-term effects of *Padi4* deletion in the haematopoietic system, we carried out immunophenotypic analyses of *Padi4*^{CKO} mice aged up to 1 year, as well as BM reconstitution experiments using HSCs from these aged mice (Figure 5A,B). Analysis of BM and spleens of 1 year-old *Padi4*^{CKO} mice and *Padi4*^{CTL} mice showed no difference in cell counts of total WBC, primitive LSK compartments, LK progenitor populations or differentiated cell populations (Figure 5A). In addition, *in vitro* CFC assays using aged BM from *Padi4*^{CKO} and *Padi4*^{CTL} mice also showed no difference in CFC colony count between the genotypes (Figure 5A). In fact, the differences observed in young mice (Figure 1C,D,E,H) were not observed upon ageing. To assess the self-renewal potential of aged *Padi4*^{CKO} HSCs, we transplanted sorted HSCs from 1-year old *Padi4*^{CKO} and *Padi4*^{CTL} mice into primary recipients and analysed the bone marrow of the recipients at 36 weeks post-transplantation. Mice transplanted with *Padi4*^{CKO} HSCs showed a small decrease in the contribution of donor derived CD45.2⁺ cells to the LK and HPC1 progenitor populations as well as a decrease in differentiated granulocytes (Figure 5B). No differences in the ability of *Padi4*^{CKO} HSCs to contribute to spleen or peripheral blood cells was found (Figure 5B and Supplementary Figure 5). Taken together, these

results show that *Padi4* loss does not significantly affect long-term cell-autonomous HSC maintenance and normal haematopoiesis.

Discussion

This study demonstrates that the nuclear peptidylarginine deiminase PADI4, which is most highly expressed in the bone marrow and peripheral blood, is not required for cell-autonomous steady-state haematopoiesis, long-term self-renewal of HSCs, efficient reconstitution of multi-lineage haematopoiesis in serial transplantation assays or response of HSCs to haematopoietic injury. Histone citrullination is antagonistic to histone arginine methylation (Cuthbert *et al.*, 2004; Wang *et al.*, 2004), a modification that has established roles in the regulation of haematopoiesis (Kolodziej *et al.*, 2014; Greenblatt, Liu and Nimer, 2016) and PADI4 was previously shown to influence gene expression by counteracting arginine methylation in erythroleukaemia cells (Kolodziej *et al.*, 2014). As a result, PADI4 was proposed to modulate lineage specification of haematopoietic stem and progenitor cells (Kolodziej *et al.*, 2014). However, our *in vivo* data show that genetic *Padi4* deletion does not have a significant effect on haematopoiesis. PADI4 is widely deregulated in cancer development (Chang and Han, 2006). Collectively, these findings suggest that deregulated, but not physiological, PADI4 levels can interfere with histone arginine methylation-regulated gene regulation in the haematopoietic system. A previous study conducted using *Padi4*-null mice (Nakashima *et al.*, 2013) suggested that PADI4 regulates the proliferation of multipotent stem cells in the BM, as such mice showed increased numbers of LSK cells. Our experiments using haematopoiesis-specific deletion of *Padi4* replicate this phenotype, but show that it does not translate into effects in any measurable aspect of haematopoiesis.

The results presented here have significant implications for biomedicine. PADI4 is expressed in HSCs, down-regulated upon differentiation to committed haematopoietic progenitors and up-regulated in leukaemia stem cells during the development of acute myeloid leukaemia (Figure 1A and (Krivtsov *et al.*, 2006)). Furthermore, it was shown to act as a co-activator of Tal1, a key transcriptional regulator in the development of T-cell acute lymphoblastic leukaemia (Chen *et al.*, 1990; Kolodziej *et al.*, 2014). PADI4 is therefore a promising target for the treatment of leukaemia and our results indicate that targeting it may offer a therapeutic window. Most pertinently, significant efforts are currently underway to develop PADI4 inhibitors for the treatment of rheumatoid arthritis, systemic lupus erythematosus, atherosclerosis, thrombosis, irritable bowel syndrome, and colon cancer (Lewis and

Nacht, 2016). The fact that ablation of *Padi4* does not lead to impairment in the functions of the haematopoietic system, where it is most highly expressed, suggests that systemic PADI4 inhibition may be administered without adverse effects.

Materials and Methods

Mice. All experiments on animals were performed under UK Home Office authorisation. All mice were of C57BL/6 genetic background. *Padi4*^{fl/fl} mice (Hemmers *et al.*, 2011) were a kind gift from the Mowen lab. *Vav-iCre* and *Mx1-Cre*, have been described previously (Kühn *et al.*, 1995; de Boer *et al.*, 2003; Vukovic *et al.*, 2015). All transgenic and knockout mice were CD45.2⁺. Congenic recipient mice were CD45.1⁺/CD45.2⁺. Sex-matched 8 to 12 week-old mice were used throughout. All experiments on mice were performed under University of Edinburgh's Veterinary oversight with UK Home Office authorization.

Flow cytometry. All BM cells were prepared and analyzed as described previously (Kranc *et al.*, 2009; Mortensen *et al.*, 2011; Guitart *et al.*, 2013, 2017; Vukovic *et al.*, 2015). BM cells were isolated by crushing tibias and femurs using a pestle and mortar. Cell suspensions were passed through a 70µm strainer. PB was collected in EDTA coated microvettes. Spleen and thymus were homogenised and passed through a cell strainer. Single cell suspensions were incubated with Fc block and then stained with antibodies. For HSC cell analyses, unfractionated BM cells were stained with a lineage marker cocktail containing biotin-conjugated anti-CD4, anti-CD5, anti-CD8a, anti-CD11b, anti-B220, anti-Gr-1 and anti-Ter119 antibodies together with APC-conjugated anti-c-Kit, FITC-conjugated anti-Sca-1, PE-conjugated anti-CD48 and PE-Cy7-conjugated anti-CD150 antibodies. Biotin-conjugated antibodies were then stained with Pacific Blue-conjugated streptavidin. For pan-lineage progenitor cell staining, cells were stained with the lineage marker cocktail described above together with APC-conjugated anti-c-kit, PE-Cy7-conjugated anti-Sca-1, BV-421-conjugated anti-CD127, FITC-conjugated anti-CD34, PE-conjugated anti-CD135 and APC-Cy7-conjugated anti-CD16/32. For myeloid/T lymphoid restricted progenitors, cells were stained with a lineage marker cocktail containing biotin-conjugated anti-CD4, anti-CD5, anti-CD8a, anti-Mac-1, anti-B220, anti-CD19 and anti-Gr-1 together with BV-510-conjugated anti-c-kit, Pacific Blue-conjugated anti-Sca-1, PE-Cy7-conjugated anti-CD150, APC-Cy7-conjugated anti-CD16/32, APC-conjugated anti-CD41, PE-conjugated anti-CD105 and FITC-conjugated anti-Ter119. Biotin-conjugated antibodies were then stained with PerCP-conjugated streptavidin. For analyses of differentiated cells, spleen, BM or PB cell suspensions

were stained with APC-Cy7-conjugated anti-CD19 antibody for B cells; Pacific Blue-conjugated anti-CD11b and PE-Cy7-conjugated anti-Gr-1 for myeloid cells; APC-conjugated anti-CD8 antibodies and PE-conjugated anti-CD4 antibodies for T cell analysis (spleen and PB); FITC-conjugated anti-Ter119 and PE-conjugated anti-CD71 (BM).

To distinguish CD45.2⁺-donor derived cells in the BM and spleen of transplanted mice, BV711-conjugated anti-CD45.1 and Pacific Blue-conjugated anti-CD45.2 antibodies were used. For HSC staining in transplanted mice, the remainder of the staining was as described above. For analyses of differentiated cells in BM and spleen of transplanted mice, myeloid cells were stained with PE-conjugated anti-CD11b, PE-Cy7-conjugated anti-Gr-1 and FITC-conjugated anti-Ter119 for erythroid cells. B Lymphoid cells were stained with APC-Cy7-conjugated anti-CD19. PB of transplanted mice was stained with FITC-conjugated anti-CD45.1, Pacific Blue-conjugated anti-CD45.2, PE-conjugated anti-CD4 and CD8a, PE-Cy7-conjugated anti-Gr-1, APC-conjugated anti-CD11b, and APC-Cy7-conjugated anti-CD19.

The catalogue numbers, clone numbers and manufacturer information for the above antibodies is provided in Supplementary Table 1.

Flow cytometry analyses were performed using a LSRFortessa (BD). Cell sorting was performed on a FACSAria Fusion (BD).

Colony forming cells (CFC) assays. CFC assays were carried out using MethoCult™ M3434 (STEMCELL Technologies) methylcellulose medium (Lawson *et al.*, 2021a,b); . Two technical replicates were used per each biological replicate in each experiment. BM cells were plated for 10 days before colony types were identified and counted.

Blood profiling. Blood was collected via cardiac puncture into an EDTA coated microvette and analysed on a Celltaq Haematology analyser (Nihon Kohden).

Syngeneic transplantation assays. CD45.1⁺/CD45.2⁺ C57BL/6 recipient mice were lethally irradiated using a split dose of 11 Gy (two doses of 5.5 Gy administered at least 4 hours apart) at an average rate of 0.58 Gy/min using a Cesium 137 GammaCell 40 irradiator (Mapperley *et al.*, 2020). For primary transplantations 200 LSKCD48⁺CD150⁺ HSCs (per recipient) sorted from BM of the donor mice were mixed with 200,000 unfractionated support CD45.1⁺ wild type BM cells and

transferred into lethally irradiated CD45.1⁺/CD45.2⁺ recipients. For secondary transplantations 2,000-3,000 CD45.2⁺ LSK cells sorted from BM of primary recipients were mixed with 200,000 unfractionated support CD45.1⁺ wild-type BM cells and re-transplanted. For all except ageing experiments, primary and secondary recipients were culled and analysed 16-20 weeks post transplant.

Poly I:C administration. Both *Padi4*^{CTL} and *Padi4*^{KO} (*Padi4*;Mx1-Cre) transgenic and CD45.1⁺/CD45.2⁺ C57BL/6 recipient mice were injected intraperitoneally with poly I:C. *Padi4*^{CTL} and *Padi4*^{KO} mice received 6 injections of 300 µg Poly I:C, on every other day. Mice were culled and analysed 1 month following the final administration. Recipient mice received one injection every other day with 300 µg Poly I:C (GE Healthcare) for a total of 6 doses starting 8 weeks after transplantation as previously described (Kranc *et al.*, 2009; Guitart *et al.*, 2013, 2017).

5-FU administration. Both *Padi4*^{CTL} and *Padi4*^{CKO} transgenic mice were injected intraperitoneally with 5-FU. Mice were weighed on the day of administration and received 3 injections of 150 mg/kg 10 days apart. Mice were culled and analysed 10 days following the final administration.

Western blotting. Proteins extracted from *Padi4*^{CTL} and *Padi4*^{CKO} were subjected to SDS-PAGE (4–20% Mini-PROTEAN[®] TGX[™] Precast gel, Biorad) and then transferred onto a nitrocellulose membrane. Membranes were blocked in 5% BSA-TBST (TBS with 0.1% Tween20) and probed with anti-Padi4 (Abcam ab214810, 1:1000, O/N at 4°C) and anti-Actin (Santa Cruz, sc-1616, 1:500, O/N at 4°C). After incubation with appropriate horseradish peroxidase-coupled secondary antibody, proteins were detected with SuperSignal[™] West Pico PLUS Chemiluminescent Substrate (ThermoFisher Scientific) and acquired on the ImageQuant LAS (GE Healthcare Life Sciences).

Transcriptomic analyses

Expression data were derived from multiple bulk-sequencing datasets from ArrayExpress and NCBI GEO. Each study, identified by accession number, contributed data to multiple populations as follows: E-MTAB-1963 (LSK, CMP); E-MTAB-3079 (LSK, CLP, CMP, GMP); E-MTAB-2262 (HSC, MPP1, MPP2, MPP3, MPP4); GSE116177 (LSK, CLP, CMP, GMP); GSE125846 (HSC, CMP, GMP, MEP). Data were aligned to the GRCm38 mouse genome using hisat2, and inter-study batch correction was performed using the batchelor package in R, after which FPKM expression values were computed and plotted.

Genotyping. DNA was extracted from bone marrow taken from recipient mice transplanted with *Padi4*^{CTL}, *Padi4*^{CKO} or *Padi4*^{KO} mice. PCR was performed using primers specific for *Padi4* deletion. Forward primer: 5'-CAG GAG GTG TAC GTG TGC A-3'. Reverse primer: 5'-AGT CCA GCT GAC CCT GAA C-3'. Expected band sizes: Wild-type *Padi4* allele: 104bp; Floxed *Padi4* allele: 160bp; Knock-out *Padi4* allele: 215bp.

Statistical analysis. Statistical significance was determined using Mann-Whitney or One-Way ANOVA on Graphpad V 8 software.

Author contributions

M.A.C. conceived the study. M.A.C. and K.R.K. planned the experiments, supervised the work and wrote the manuscript. C.Y. performed all of the experiments and data analysis. J.R.R., H.L. and C.M. provide assistance with sample collection and experiment execution. L.N.VDL. performed bioinformatics analyses of RNA-sequencing datasets.

Acknowledgements

We thank the flow cytometry and mouse facilities at the Scottish Centre for Regenerative Medicine. We thank M. Dawson for useful discussions at the conception stage of the project and members of the Christophorou and Kranc labs for critical discussions of the work.

Funding

This work was funded by a Wellcome Trust and Royal Society Sir Henry Dale Fellowship to M.A.C. (Grant No. 105642/Z/14/Z). K.R.K's laboratory is funded by a Cancer Research UK program grant (C29967/A26787) and project grants from the Medical Research Council, Blood Cancer UK, Barts Charity, and the Kay Kendall Leukaemia Fund.

Data availability

Gene expression data were derived from multiple bulk-sequencing datasets from ArrayExpress and NCBI GEO. Each study, identified by accession number, contributed data to multiple populations as follows: E-MTAB-1963 (LSK, CMP); E-MTAB-3079 (LSK, CLP, CMP, GMP); E-MTAB-2262 (HSC, MPP1, MPP2, MPP3, MPP4); GSE116177 (LSK, CLP, CMP, GMP); GSE125846 (HSC, CMP, GMP, MEP).

The authors declare no competing interests.

References

Arita, K. *et al.* (2004). Structural basis for Ca²⁺-induced activation of human PAD4. *Nature Structural and Molecular Biology*. **11**(8), 777–783.

de Boer, J. *et al.* (2003). Transgenic mice with hematopoietic and lymphoid specific expression of Cre. *European Journal of Immunology*. **33**(2), 314-25.

Buza-Vidas, N. *et al.* (2011). GATA3 is redundant for maintenance and self-renewal of hematopoietic stem cells. *Blood*. **118**(5), 1291–1293.

Chan, R. J. *et al.* (2003). A definitive role of Shp-2 tyrosine phosphatase in mediating embryonic stem cell differentiation and hematopoiesis. *Blood*. **102**(6), 2074–2080.

Chang, X. and Han, J. (2006). Expression of Peptidylarginine Deiminase Type 4 (PAD4) in Various Tumors. *Molecular Carcinogenesis*. **45**,183–196.

Chen, M. J. *et al.* (2009). Runx1 is required for the endothelial to haematopoietic cell transition but not thereafter. *Nature*, **457**(7231). 887–891.

Chen, Q. *et al.* (1990). The tal gene undergoes chromosome translocation in T cell leukemia and potentially encodes a helix-loop-helix protein. *EMBO Journal*. **9**, 415-424.

Christophorou, M. A. *et al.* (2014) Citrullination regulates pluripotency and histone H1 binding to chromatin. *Nature*. **507**(7490), 104–108.

Cuthbert, G. L. *et al.* (2004). Histone deimination antagonizes arginine methylation. *Cell*. **118**(5), 545–553.

Greenblatt, S. M., Liu, F. and Nimer, S. D. (2016). Arginine methyltransferases in normal and malignant hematopoiesis. *Experimental Hematology*. **44**(6), 435-41.

Guitart, A. V. *et al.* (2013). Hif-2 α is not essential for cell-autonomous hematopoietic stem cell maintenance. *Blood*. **122**(10), 1741–1745.

Guitart, A. V. *et al.* (2017). Fumarate hydratase is a critical metabolic regulator of hematopoietic stem cell functions. *The Journal of Experimental Medicine*. **214**(3), 719–735.

Guo, Q. and Fast, W. (2011). Citrullination of Inhibitor of Growth 4 (ING4) by Peptidylarginine Deminase 4 (PAD4) disrupts the interaction between ING4 and p53. *Journal of Biological Chemistry*. **286**(19), 17069–17078.

Hemmers, S. *et al.* (2011). PAD4-mediated neutrophil extracellular trap formation is not required for immunity against influenza infection. *PLoS ONE*. **6**(7), e22043.

Jasper, de B. *et al.* (2003). Transgenic mice with hematopoietic and lymphoid specific expression of Cre. *European Journal of Immunology*. **33**(2), 314–325.

Kolodziej, S. *et al.* (2014). PADI4 acts as a coactivator of Tal1 by counteracting repressive histone arginine methylation. *Nature Communications*. **5**, 3995.

Kranc, K. R. *et al.* (2009). Cited2 Is an Essential Regulator of Adult Hematopoietic Stem Cells. *Cell Stem Cell*. **5**(6), 659–665.

Krivtsov, A. V. *et al.* (2006) Transformation from committed progenitor to leukaemia stem cell initiated by MLL-AF9. *Nature*. **442**(7104), 818–822.

Kühn, R. *et al.* (1995). Inducible gene targeting in mice. *Science*. **269**(5229), 1427–1429.

Lawson, H. *et al.* (2021). CITED2 coordinates key hematopoietic regulatory pathways to maintain the HSC pool in both steady-state hematopoiesis and transplantation. *Stem Cell Reports*. **16**(11), 2784-2797.

Lawson, H. *et al.* (2021). JMJD6 promotes self-renewal and regenerative capacity of hematopoietic stem cells. *Blood Advances*. **5**(3), 889-899.

Lewis, H. D. and Nacht, M. (2016). IPAD or PADi - “tablets” with therapeutic disease potential? *Current Opinion in Chemical Biology*. **33**, 169-78.

Liu, F. *et al.* (2015). Arginine methyltransferase PRMT5 is essential for sustaining normal adult hematopoiesis. *Journal of Clinical Investigation*. **125**(9), 3532–3544.

Loizou, J. I. *et al.* (2009). Histone Acetyltransferase Cofactor Trrap Is Essential for Maintaining the Hematopoietic Stem/Progenitor Cell Pool. *The Journal of Immunology*. **183**(10), 6422–6431.

Mapperley, C. *et al.* (2020). The mRNA m⁶A reader YTHDF2 suppresses proinflammatory pathways and sustains hematopoietic stem cell function. *J Exp Med*. **218**(3), e20200829.

Mortensen, M. *et al.* (2011). The autophagy protein Atg7 is essential for hematopoietic stem cell maintenance. *Journal of Experimental Medicine*. **208**(3), 455–467.

Musse, A. A. *et al.* (2008). Peptidylarginine deiminase 2 (PAD2) expression in a transgenic mouse leads to specific central nervous system (CNS) myelin instability. *Disease Models and Mechanisms*. **1**(4), 229–240.

Nakashima, K. *et al.* (2013). PAD4 regulates proliferation of multipotent haematopoietic cells by controlling c-myc expression. *Nature Communications*. **4**, 1836.

Nakashima, K., Hagiwara, T. and Yamada, M. (2002). Nuclear localization of peptidylarginine deiminase V and histone deimination in granulocytes. *Journal of Biological Chemistry*. **277**(51), 49562-8.

Ogilvy, S. *et al.* (1999). Promoter elements of vav drive transgene expression in vivo throughout the hematopoietic compartment. *Blood*. **94**(6), 1855–63.

Ou, X. *et al.* (2011). SIRT1 deficiency compromises mouse embryonic stem cell hematopoietic differentiation, and embryonic and adult hematopoiesis in the mouse. *Blood*. **117**(2), 440–450.

Paris, J. *et al.* (2019). Targeting the RNA m⁶A Reader YTHDF2 Selectively Compromises Cancer Stem Cells in Acute Myeloid Leukemia. *Cell Stem Cell*. **25**(1), 137-148.

Shimshek, D. R. *et al.* (2002). Codon-improved Cre recombinase (iCre) expression in the mouse. *Genesis*. **32**(1), 19–26.

Slade, D. J. *et al.* (2015). Protein arginine deiminase 2 binds calcium in an ordered fashion: Implications for inhibitor design. *ACS Chemical Biology*. **10**(4), 1043–1053.

Stadler, S. C. *et al.* (2013). Dysregulation of PAD4-mediated citrullination of nuclear GSK3 β activates TGF- β signaling and induces epithelial-to-mesenchymal transition in breast cancer cells. *Proceedings of the National Academy of Sciences of the United States of America*. **110**(29), 11851-6.

Suzuki, A. *et al.* (2003). Functional haplotypes of PADI4, encoding citrullinating enzyme peptidylarginine deiminase 4, are associated with rheumatoid arthritis. *Nature Genetics*. **34**(4), 395–402.

Tanikawa, C. *et al.* (2009). Regulation of protein citrullination through p53/PADI4 Network in DNA damage response. *Cancer Research*. **69**(22), 8761–8769.

Tanikawa, C. *et al.* (2018). Citrullination of RGG Motifs in FET Proteins by PAD4 Regulates Protein Aggregation and ALS Susceptibility. *Cell Reports*. **22**(6), 1473–1483.

Thieme, S. *et al.* (2013). The histone demethylase UTX regulates stem cell migration and hematopoiesis. *Blood*. **121**(13), 2462–2473.

Vossenaar, E. R. *et al.* (2004). Expression and activity of citrullinating peptidylarginine deiminase enzymes in monocytes and macrophages. *Annals of the Rheumatic Diseases*. **63**(4), 373-81.

Vukovic, M. *et al.* (2015). Hif-1 α and Hif-2 α synergize to suppress AML development but are dispensable for disease maintenance. *Journal of Experimental Medicine*. **212**(13), 2223–2234.

Wang, S. and Wang, Y. (2013). Peptidylarginine deiminases in citrullination, gene regulation, health and pathogenesis. *Biochimica et Biophysica Acta - Gene Regulatory Mechanisms*. **1829**(10), 1126-35.

Wang, Y. *et al.* (2004). Human PAD4 regulates histone arginine methylation levels via demethylimination. *Science*. **306**(5694), 279–283.

Wang, Y. C., Peterson, S. E. and Loring, J. F. (2014). Protein post-translational modifications and regulation of pluripotency in human stem cells. *Cell Research*. **24**(2), 143-60.

Witalison, E. E. *et al.* (2015). Molecular targeting of protein arginine deiminases to suppress colitis and prevent colon cancer. *Oncotarget*. **6**(34), 36053-62.

Yuzhalin, A. E. *et al.* (2018). Colorectal cancer liver metastatic growth depends on PAD4-driven citrullination of the extracellular matrix. *Nature Communications*. **9**(1), 4783.

Zhang, X. *et al.* (2011). Genome-Wide analysis reveals PADI4 cooperates with Elk-1 to activate C-Fos expression in breast cancer cells. *PLoS Genetics*. **7**(6), e1002112.

Figures

Figure 1

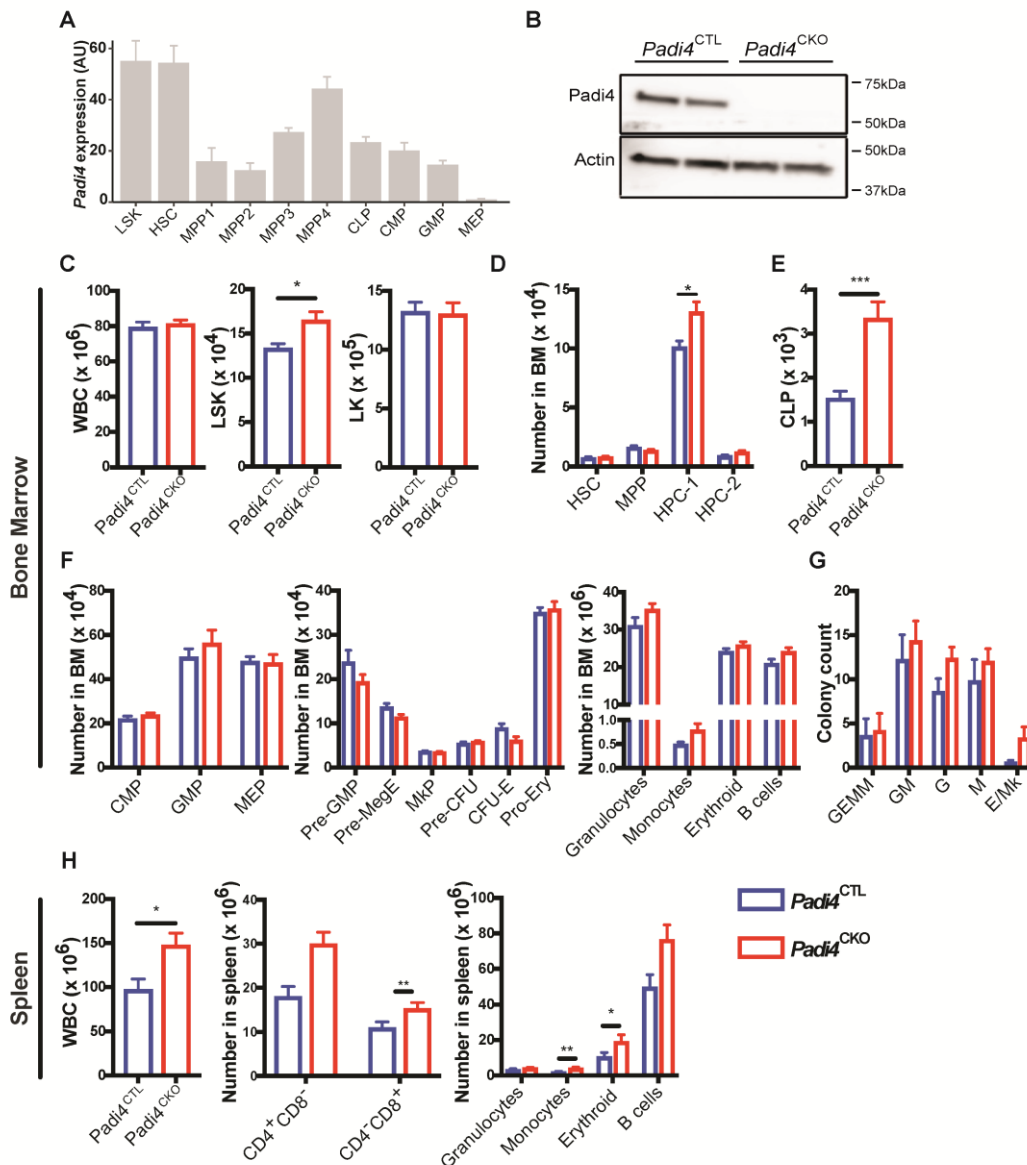


Figure 1. Haematopoiesis-specific deletion of PADI4 has no major impact on steady-state haematopoiesis. (A) Padi4 expression derived from five bulk sequencing studies and batch corrected, with each study contributing to an average of four populations. **(B)** Immunoblot analysis of mouse PADI4 in total BM extracts from *Padi4*^{CTL} and *Padi4*^{CKO} mice. Actin presented as a loading control. **(C-H)** Immunophenotypic analysis of bone marrow from 8-12 week old mice; total number of **(C)** WBC, LSK, and LK cells **(D)** HSC, MPP, HPC-1 and HPC-2 cells. *Padi4*^{CTL}, n = 9; *Padi4*^{CKO}, n = 9. **(E,F)** Total number of lymphoid, myeloid and erythroid progenitor cells. **(E)** CLP, **(F)** CMP, GMP, MEP, Pre-GMP, Pre-MegE, MkP, Pre-CFU, CFU-E,

Pro-Ery and differentiated cell populations (Granulocytes, Monocytes, Erythroid and B cells). *Padi4*^{CTL}, n = 9; *Padi4*^{CKO}, n = 9. **(G)** CFC assay with BM cells. *Padi4*^{CTL}, n = 5; *Padi4*^{CKO}, n = 6. **(H)** Immunophenotypic analysis of spleen from 8-12 week old mice; total number of WBC, T cells and differentiated cell populations (Granulocytes, Monocytes, Erythroid and B cells). *Padi4*^{CTL}, n = 9; *Padi4*^{CKO}, n = 9. All data are mean \pm SEM. *, P < 0.05; **, P < 0.01; ***, P < 0.001, ****, P < 0.0001 (Mann-Whitney U test).

Figure 2

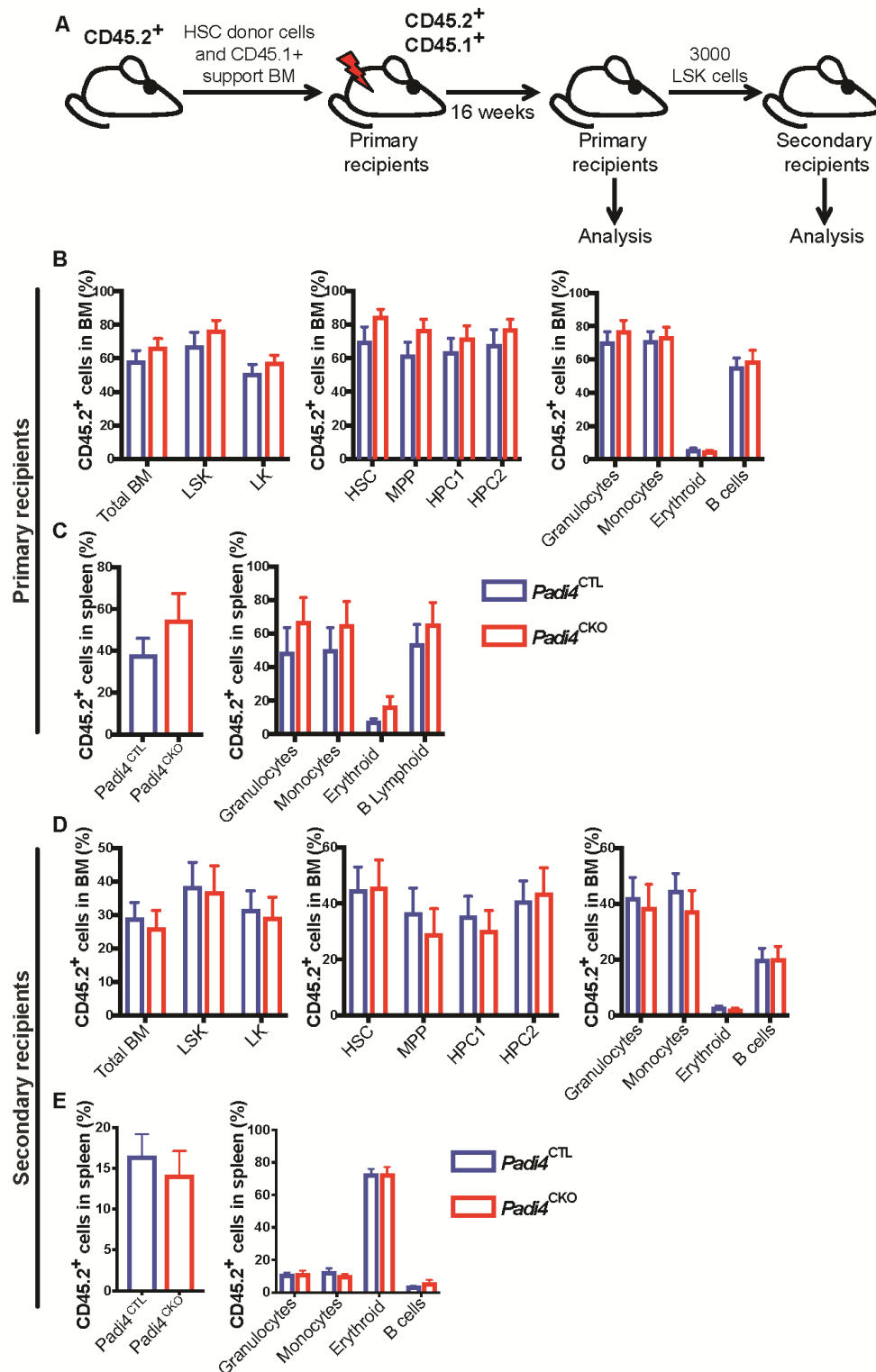


Figure 2. Haematopoiesis-specific deletion of PADI4 has no impact on BM reconstitution potential following serial transplants. (A) Experimental design for BM transplantation experiments. 200 $CD45.2^+$ BM HSCs from C57BL/6 $Padi4^{CTL}$ or $Padi4^{CKO}$ mice were transplanted into primary recipient mice and monitored for 16 weeks. Following this, a cohort of mice were sacrificed for analysis

at 16 weeks post transplantation and bone marrow was transplanted to secondary recipients. **(B)** Percentage of donor-derived CD45.2⁺ cells in total BM, LSK, LK, HSC, MPP, HPC-1, HPC-2 and differentiated cell populations (Granulocytes, Monocytes, Erythroid and B cells). *Padi4*^{CTL}, n = 14; *Padi4*^{CKO}, n = 13. **(C)** Contribution of donor-derived CD45.2⁺ cell population to total spleen WBC count and differentiated cell populations of primary recipients. *Padi4*^{CTL}, n = 6; *Padi4*^{CKO}, n = 6. **(D,E)** Secondary recipient mice were transplanted with 3000 sorted CD45.2⁺ BM LSK cells from primary recipients sacrificed at 16 weeks. **(D)** Percentage of donor-derived CD45.2⁺ cells in total BM, LSK, LK, HSC, MPP, HPC-1, HPC-1 and differentiated cell lineages (Granulocytes, Monocytes, Erythroid and B cells). *Padi4*^{CTL}, n = 19; *Padi4*^{CKO}, n = 19. 2-4 donors were used per genotype. **(E)** Contribution of donor-derived CD45.2⁺ cell population to spleen WBC and differentiated cells of secondary recipients. *Padi4*^{CTL}, n = 19; *Padi4*^{CKO}, n = 19. All data are mean ± SEM. *, P < 0.05; **, P < 0.01; ***, P < 0.001, ****, P < 0.0001 (Mann-Whitney U test).

Figure 3

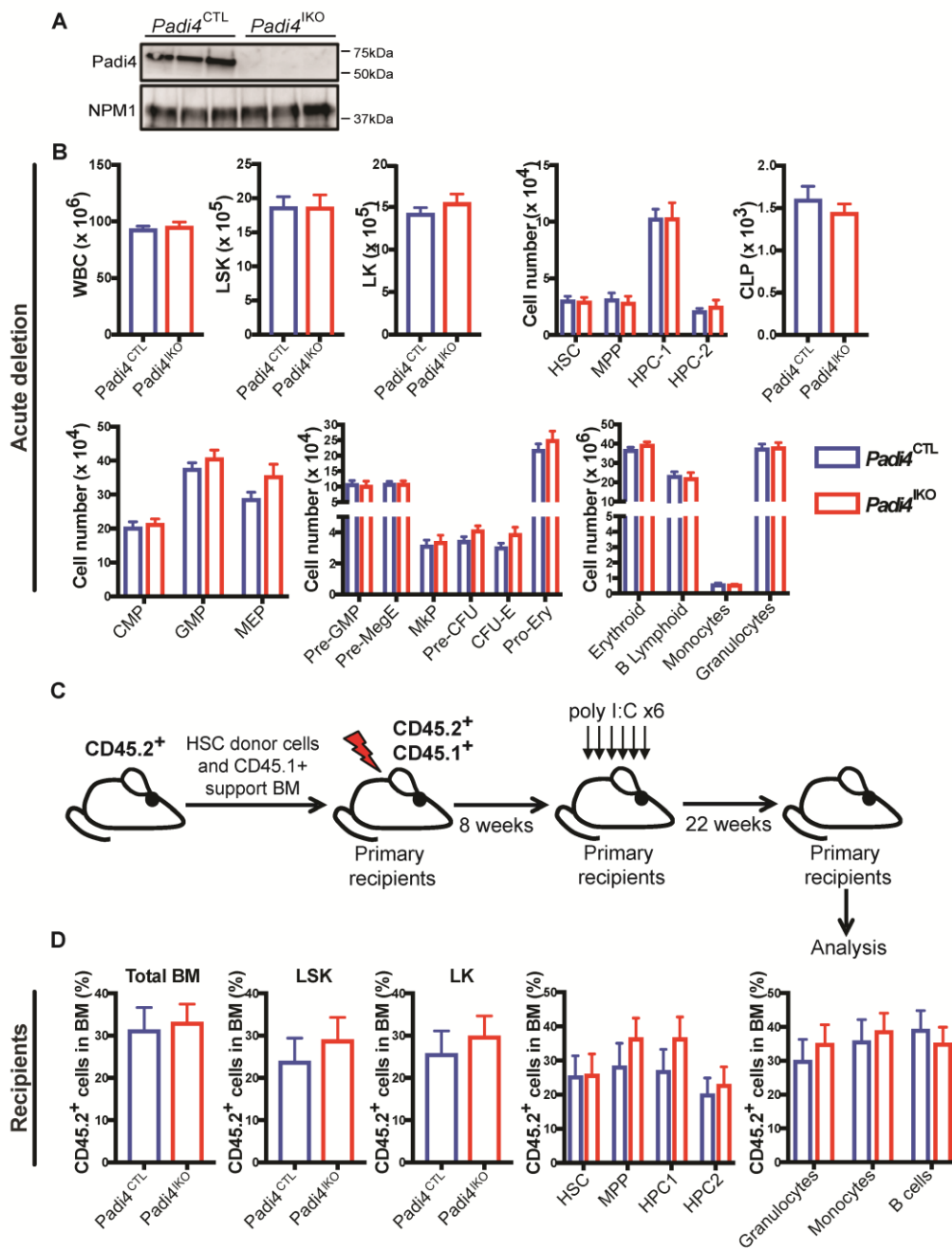


Figure 3. Acute deletion of *Padi4* in adult HSCs. *Padi4*^{CTL} and *Padi4*^{KO} mice received 6x intraperitoneal (IP) injections of Poly I:C to induce deletion of *Padi4*.

(A) Immunoblot analysis of mouse PADI4 in total BM extracts from *Padi4*^{CTL} and *Padi4*^{KO} mice. Nucleophosmin (NPM1) presented as a loading control. **(B)** Immunophenotypic analysis performed 4 weeks following the final injection. Total number of: WBC, LSK, LK, HSC, MPP, HPC-1 and HPC-2 cells; myeloid, erythroid and lymphoid progenitor cells: GMP, MEP, CMP, CLP Pre-GMP, Pre-MegE, MkP, Pre-CFU, CFU-E, Pro-Ery; differentiated granulocytes, monocytes, B cells and erythroid cells in the BM. n = 5 - 8 per genotype. **(C,D)** Transplantation of BM after

acute *Padi4* deletion. **(C)** Schematic of experimental procedure for transplantation of *Padi4*^{CTL} and *Padi4*^{KO} BM cells. 2×10^5 unfractionated CD45.2⁺ BM cells from untreated *Padi4*^{CTL} and *Padi4*^{KO} C57BL/6 (8–12 wk old) mice were mixed with 2×10^5 CD45.1⁺ WT BM cells and transplanted into lethally irradiated CD45.1⁺/CD45.2⁺ recipients. 8 wk after transplantation, the recipients received six doses of Poly I:C and the BM was analysed 22 weeks after the last injection. **(D)** Percentage of donor-derived CD45.2⁺ cells in the BM of recipient mice: LSK, LK, HSC, MPP, HPC-1, HPC-1 and differentiated cell lineages (Granulocytes, Monocytes and B cells). n = 15–21 recipients per genotype. n = 3–4 donors per genotype. All data are mean \pm SEM. *, P < 0.05; **, P < 0.01; ***, P < 0.001, ****, P < 0.0001 (Mann-Whitney U test).

Figure 4

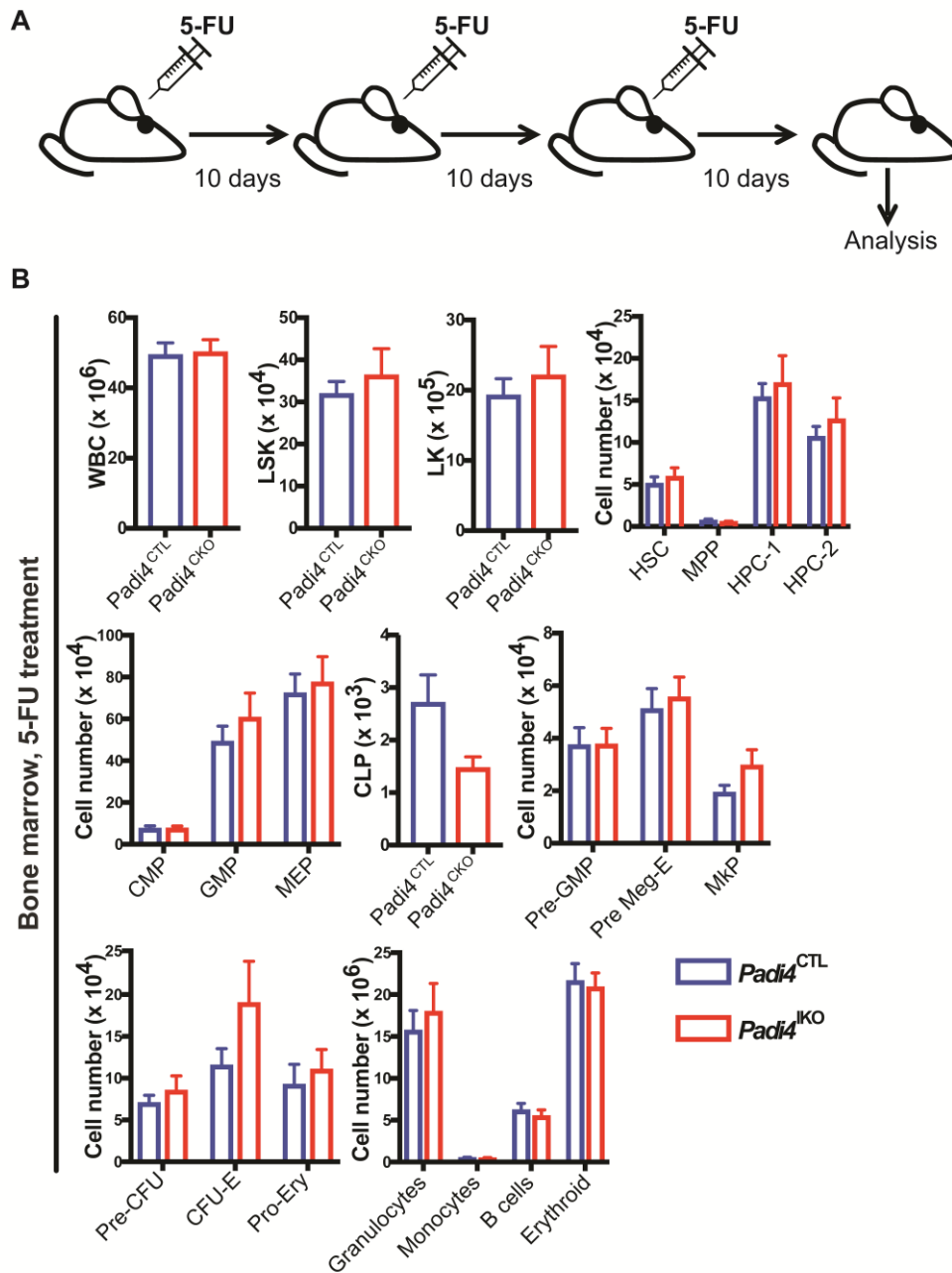
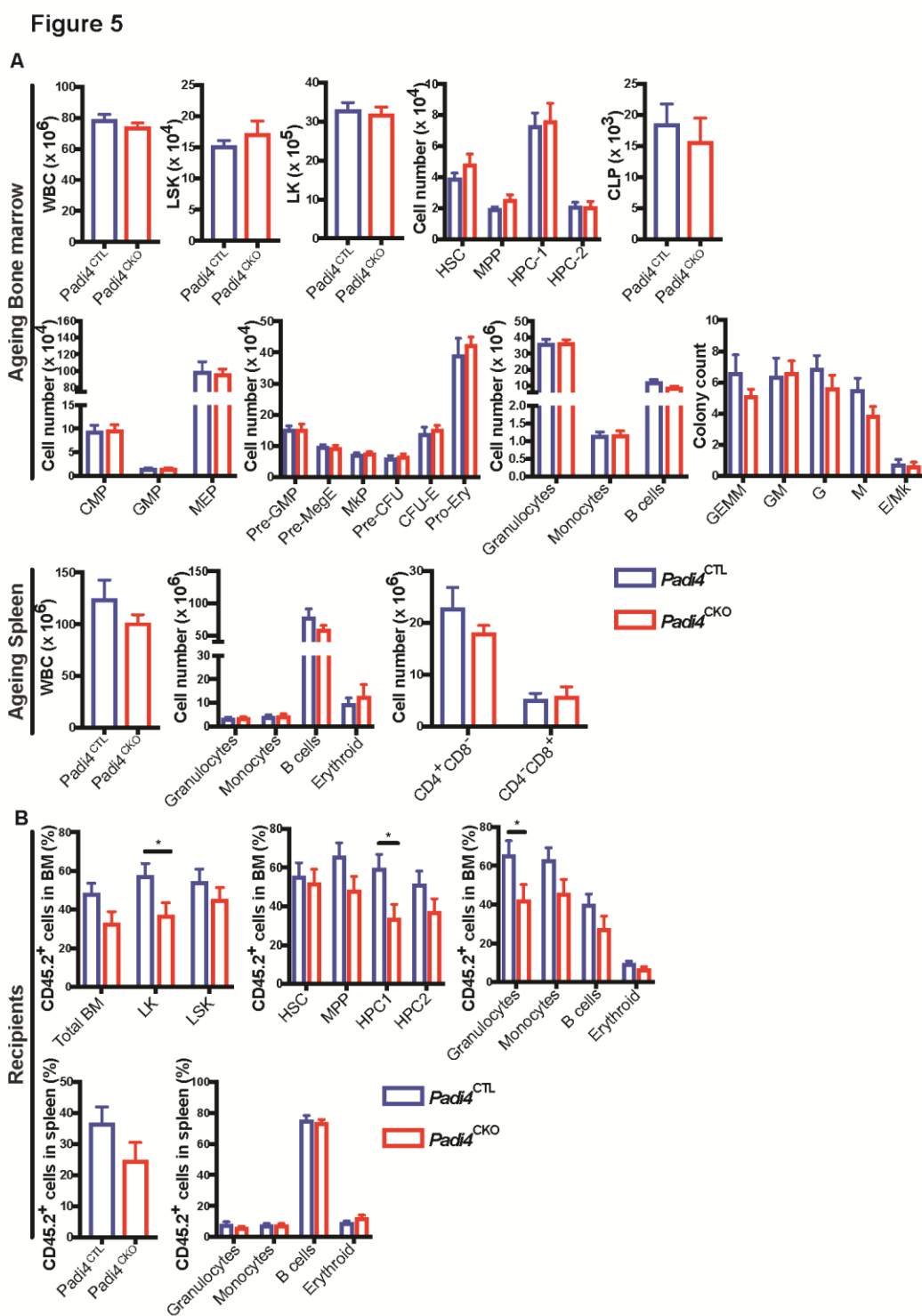


Figure 4. Assessment of *Padi4* deletion the response to haematopoietic injury.

(A) Experimental design of haematopoietic injury approach. *Padi4*^{CTL} and *Padi4*^{CKO} mice received a 3x 5-FU injections at 150 mg/kg 10 days apart and were analysed 10 days after the last administration. **(B)** Immunophenotypic analysis of *Padi4*^{CTL} and *Padi4*^{CKO} mice was performed 10 days after the final dose of 5-FU. Total number of cells in BM: WBC, LSK, and LK; HSC, MPP, HPC-1 and HPC-2 cells; myeloid, erythroid and lymphoid progenitor cells: CMP, GMP, MEP, CLP, Pre-GMP, Pre-

MegE, MkP, Pre-CFU, CFU-E, Pro-Ery; differentiated Granulocytes, Monocytes, B cells, Erythroid cells. *Padi4*^{CTL}, n = 21; *Padi4*^{CKO}, n = 18. All data are mean ± SEM. *, P < 0.05; **, P < 0.01; ***, P < 0.001, ****, P < 0.0001 (Mann-Whitney U test).



Monocytes, B cells, erythroid cells and T cells. *Padi4*^{CTL}, n = 9; *Padi4*^{CKO}, n = 8. **(B)** 200 CD45.2⁺ BM HSCs from 1 year old mice were transplanted to primary recipient mice and monitored for 24 weeks following which immunophenotypic analysis was performed on BM and spleen. Contribution of donor derived CD45.2⁺ cells to the Granulocyte, Monocyte, B cell and T cell population in PB. *Padi4*^{CTL}, n = 20; *Padi4*^{CKO}, n = 16. Percentage of donor-derived CD45.2⁺ cells in total BM, LSK, LK, HSC, MPP, HPC-1, HPC-1 and differentiated cell lineages (Granulocytes, Monocytes, B cells and erythroid cells). Contribution of donor-derived CD45.2⁺ cell population to total spleen WBC count and differentiated cell populations. *Padi4*^{CTL}, n = 17; *Padi4*^{CKO}, n = 15. 3-4 donors were used per genotype. All data are mean ± SEM. *, P < 0.05; **, P < 0.01; ***, P < 0.001, ****, P < 0.0001 (Mann-Whitney U test).

Supplementary Figure 1

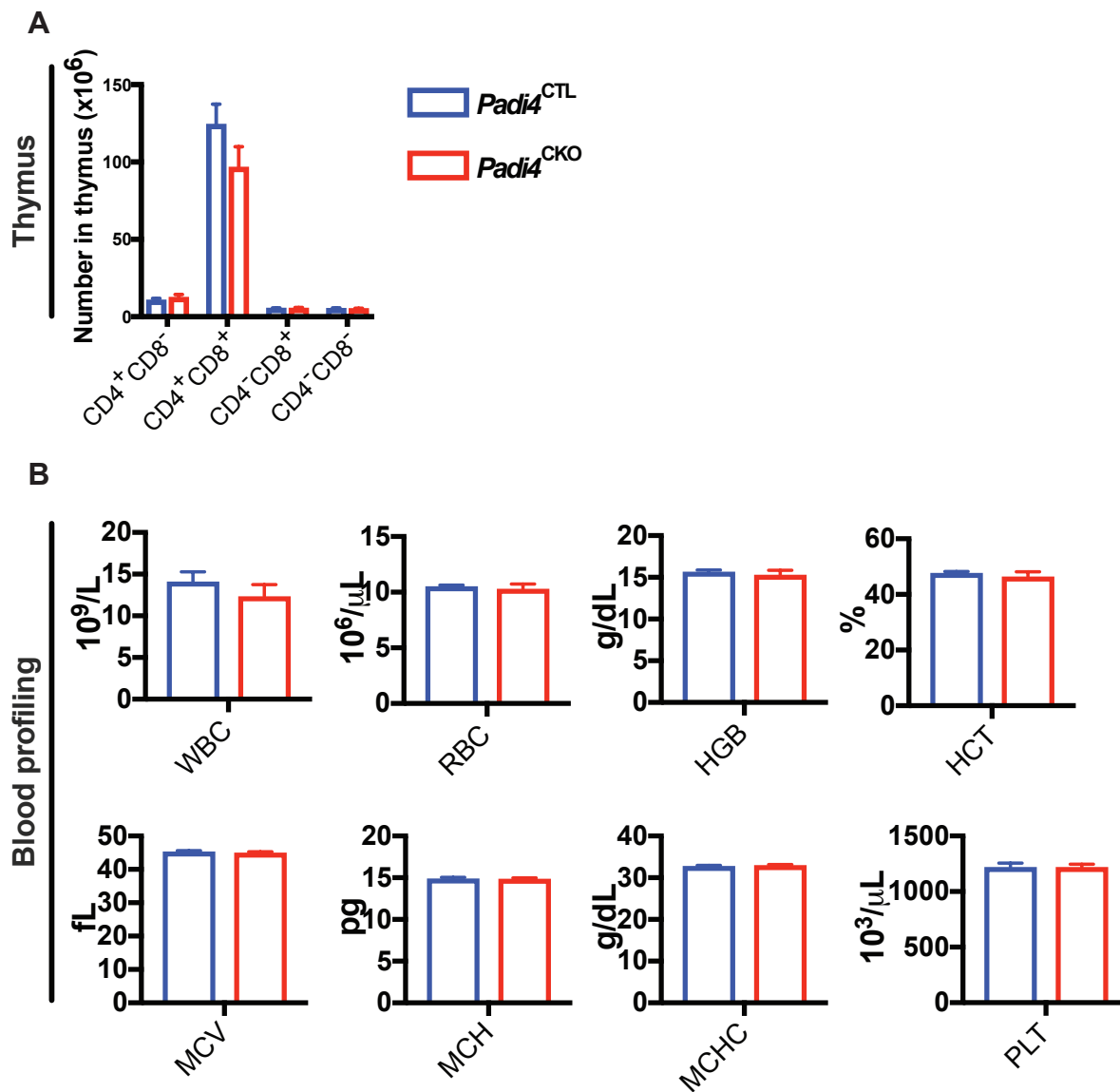


Fig. S1. Analysis of *Padi4* deletion in steady-state haematopoiesis. (A) Total number of thymic T cells. *Padi4*^{CTL}, n = 9; *Padi4*^{CKO}, n = 9. **(B)** Automated cell counting of blood samples from 8-12 week old *Padi4*^{CTL} and *Padi4*^{CKO}; WBC, RBC, HGB, HCT, MCV, MCH, MCHC and PLT counts. *Padi4*^{CTL}, n = 8; *Padi4*^{CKO}, n = 6. Data are mean \pm SEM. *, P < 0.05; **, P < 0.01; ***, P < 0.001; ****, P < 0.0001 (Mann-Whitney U test).

Supplementary Figure 2

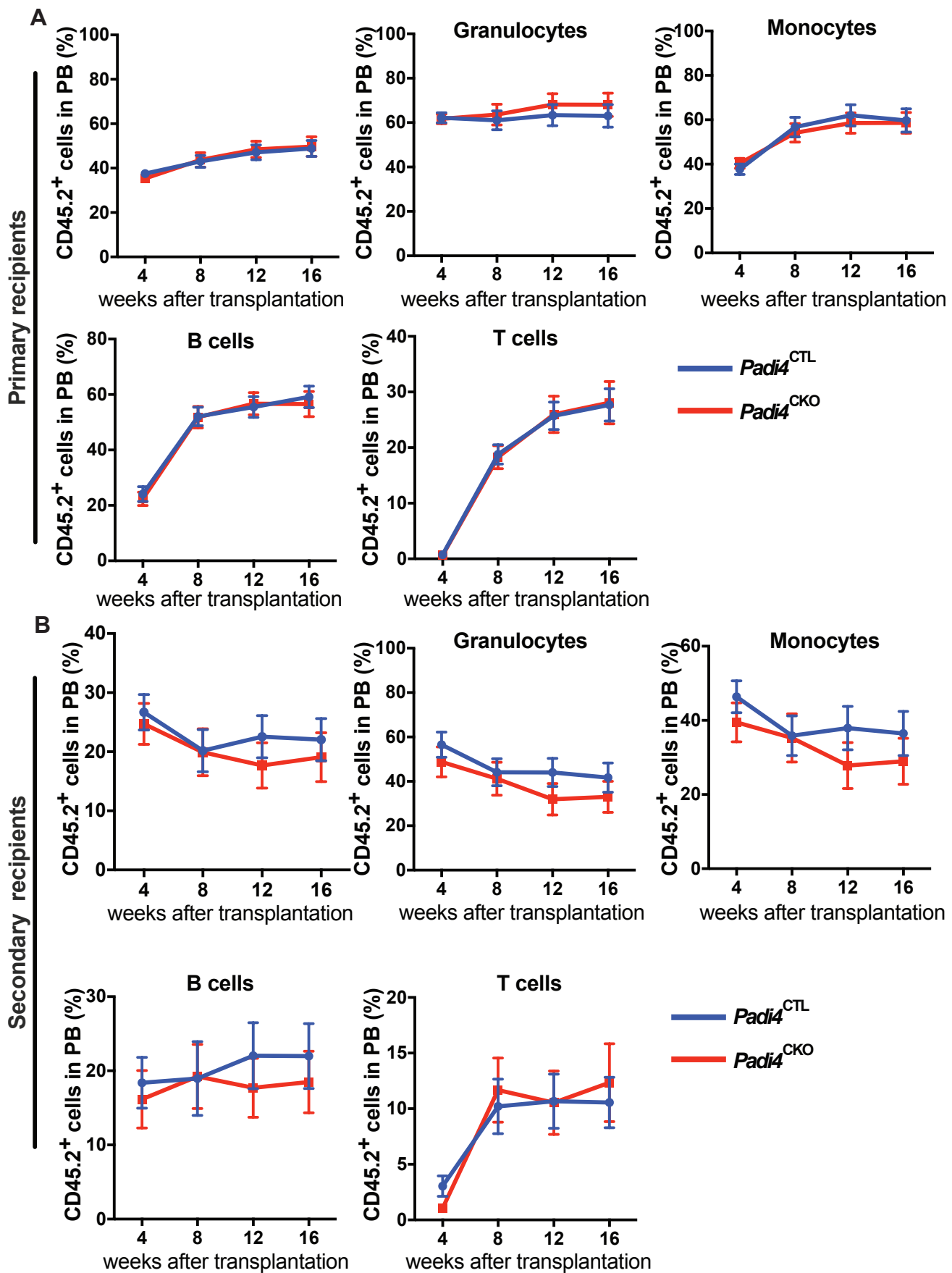


Fig. S2. Peripheral blood analysis of mice transplanted with *Padi4*^{CTL} and *Padi4*^{CKO} bone marrow. Percentage of donor-derived CD45.2⁺ cells in PB and contribution of donor derived CD45.2⁺ cells to the Granulocyte, Monocyte, B cell and T cell population in PB. **(A)** Analysis of primary recipient mice. *Padi4*^{CTL}, n = 36; *Padi4*^{CKO}, n = 34. **(B)** Secondary recipient mice. *Padi4*^{CTL}, n = 21; *Padi4*^{CKO}, n = 22. Data are mean ± SEM. *, P < 0.05; **, P < 0.01; ***, P < 0.001; ****, P < 0.0001 (Mann-Whitney U test).

Supplementry Figure 3

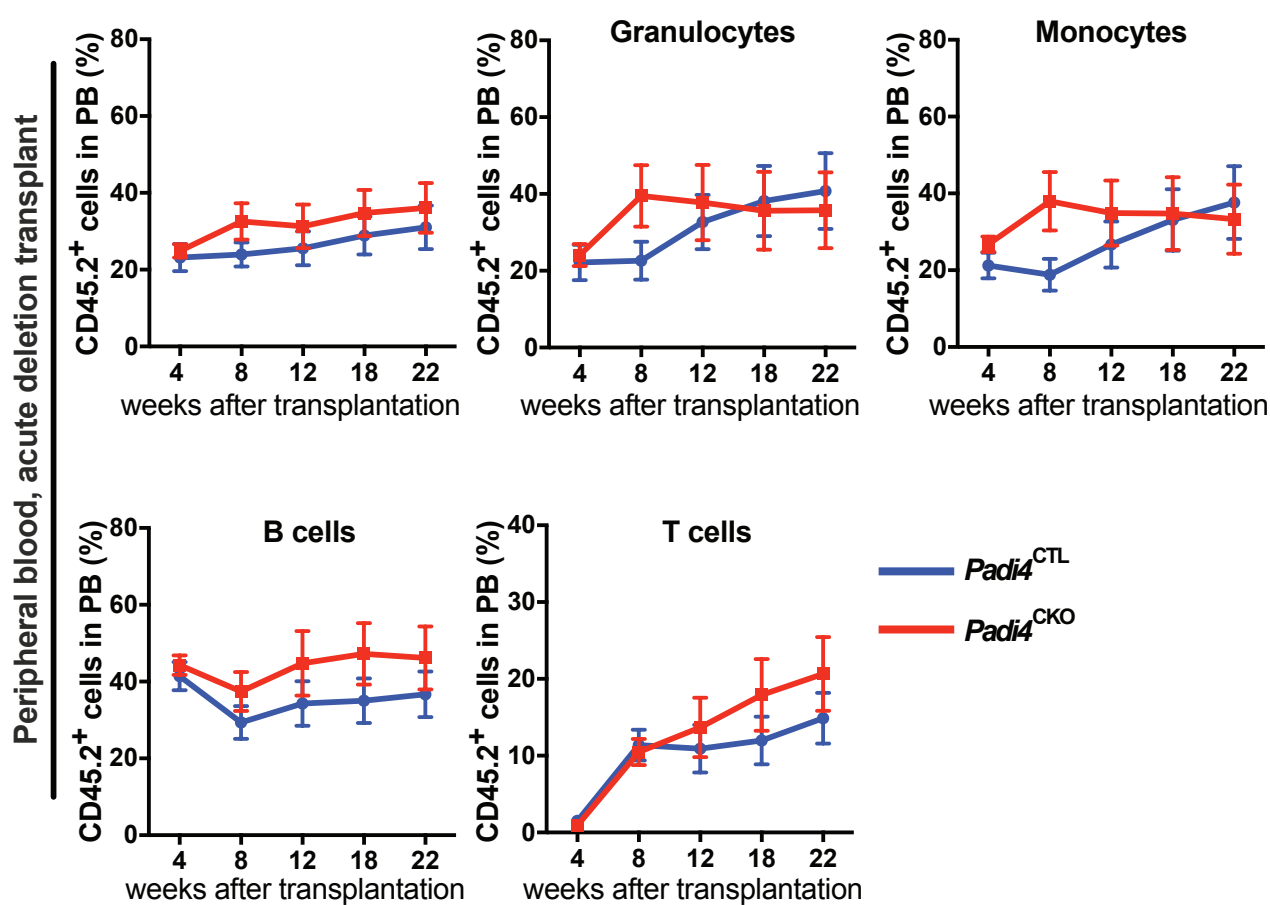


Fig. S3. Peripheral blood analysis after acute deletion of *Padi4*. Percentage of donor-derived CD45.2⁺ cells in PB and contribution of donor derived CD45.2⁺ cells to the Granulocyte, Monocyte, B cell and T cell population in PB of recipient mice, after acute deletion of *Padi4*. n = 15–21 recipients per genotype. n = 3–4 donors per genotype. Data are mean ± SEM. *, P < 0.05; **, P < 0.01; ***, P < 0.001; ****, P < 0.0001 (Mann-Whitney U test).

Supplementary Figure 4

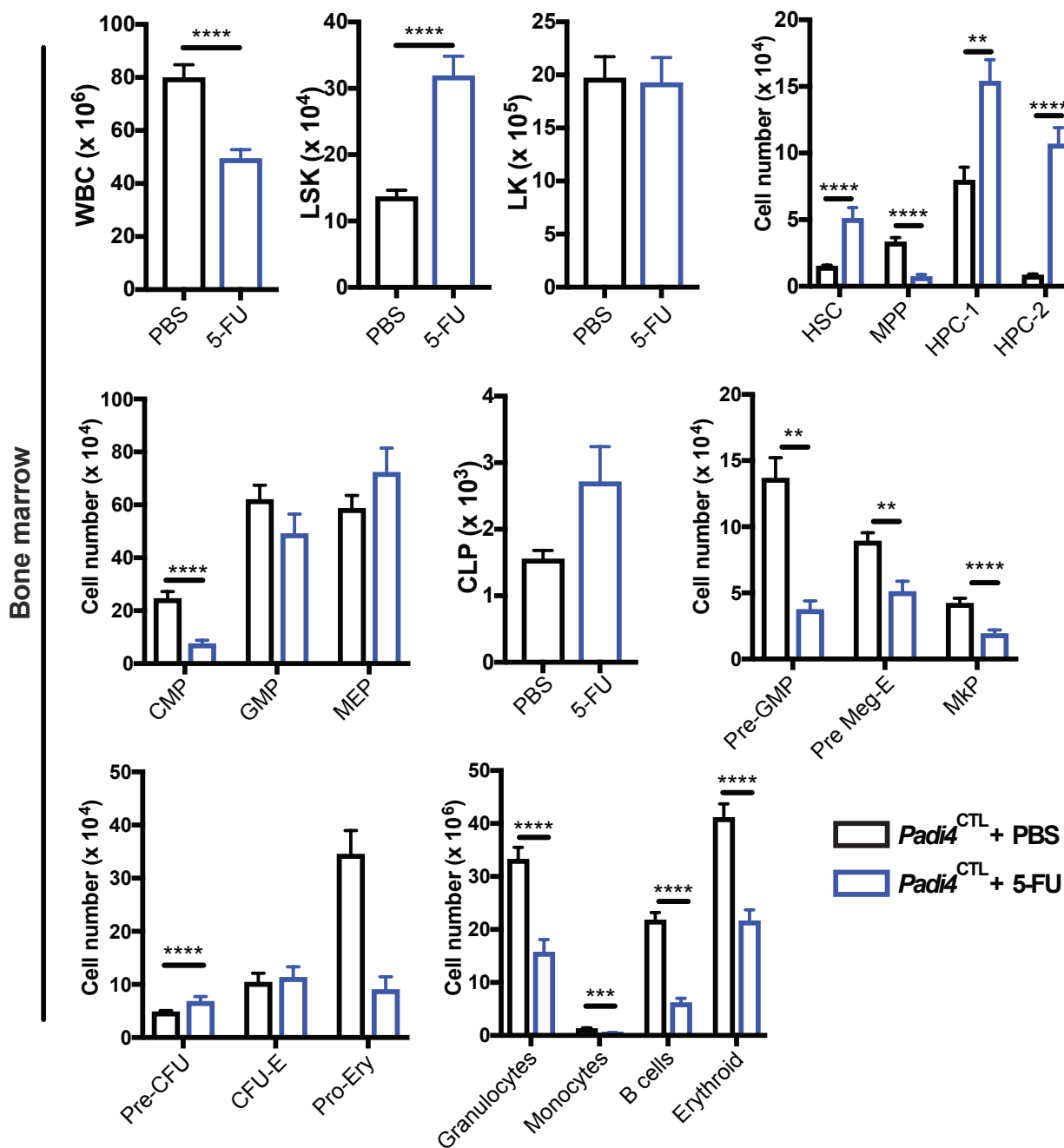


Fig. S4. 5-FU treatment leads to depletion of all bone marrow cell compartments in *Padi4*^{CTL} mice. Immunophenotypic analysis of *Padi4*^{CTL} mice treated with 5-FU or PBS vehicle control, demonstrating efficiency of 5-FU treatment. Experimental setup described in Figure 2A. Analysis was performed 10 days after the final dose of 5-FU; total number of cells in BM; WBC, LSK, and LK, HSC, MPP, HPC-1 and HPC-2 cells, myeloid, erythroid and lymphoid progenitor cells; CMP, GMP, MEP, CLP, Pre-GMP, Pre-MegE, MkP, Pre-CFU, CFU-E, Pro-Ery, differentiated Granulocytes, Monocytes, B cells, Erythroid cells and total number of cells in Spleen; WBC, B cells, Granulocytes and Monocytes *Padi4*^{CTL}, n = 21; *Padi4*^{CKO} n = 18. Data are mean ± SEM. *, P < 0.05; **, P < 0.01; ***, P < 0.001; ****, P < 0.0001 (Mann-Whitney U test).

Supplementary Figure 5

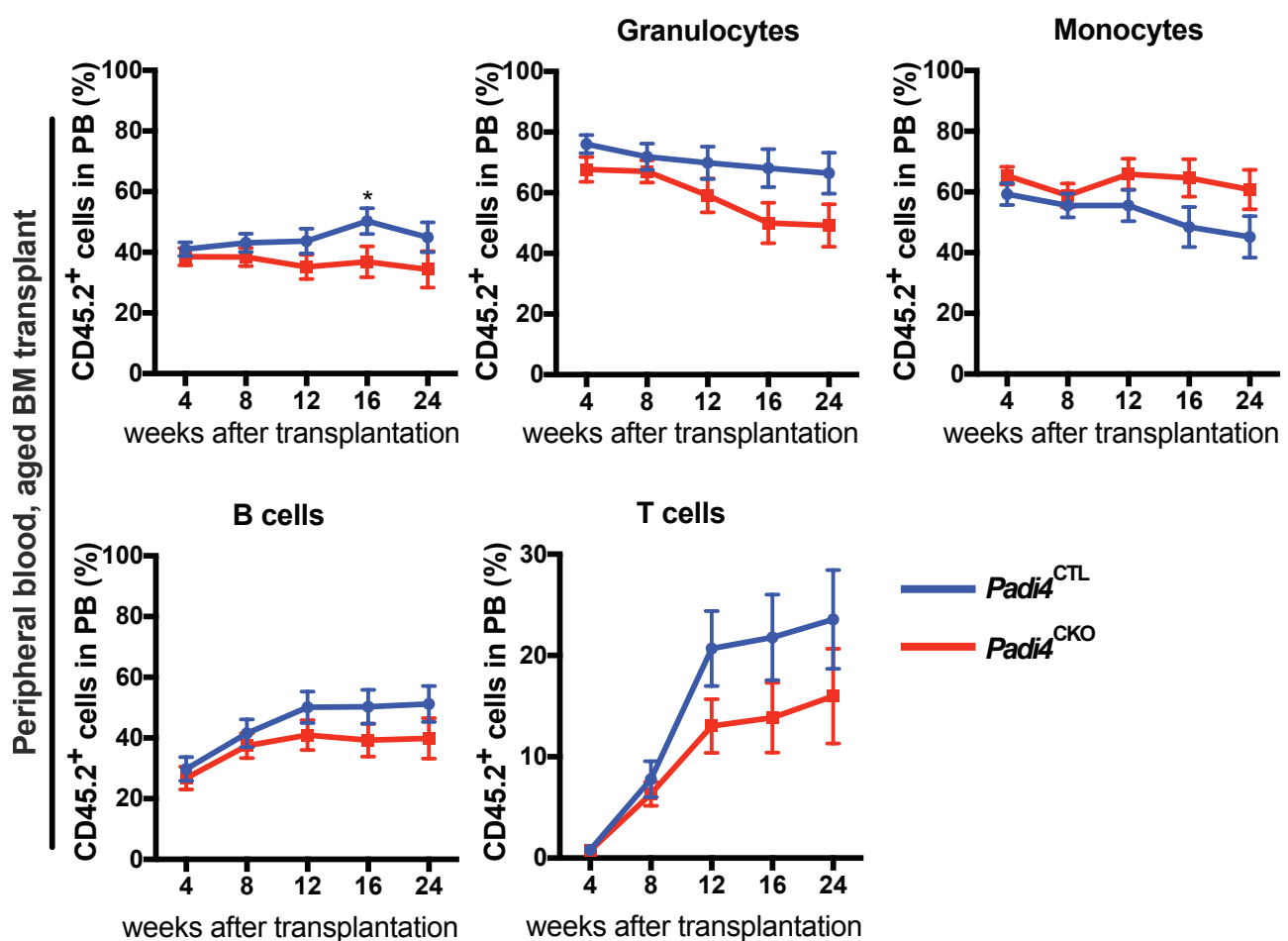


Fig. S5. Peripheral blood analysis of mice transplanted with aged *Padi4*^{CTL} and *Padi4*^{CKO} bone marrow. 200 CD45.2⁺ BM HSCs from 1 year old mice were transplanted to primary recipient mice and monitored for 24 weeks following which immunophenotypic analysis was performed on BM and spleen. Percentage of donor-derived CD45.2⁺ cells in PB. Contribution of donor derived CD45.2⁺ cells to the Granulocyte, Monocyte, B cell and T cell population in PB. *Padi4*^{CTL}, n = 20; *Padi4*^{CKO}, n = 16. Data are mean ± SEM. *, P < 0.05; **, P < 0.01; ***, P < 0.001; ****, P < 0.0001 (Mann-Whitney U test).

Table S1. List of antibodies used for flow cytometry. Antibody information for the analyses described in the Materials and Methods section *Flow Cytometry*.

Antibody	Conjugate	Catalog No.	Clone	Lot No.	Manufacturer
CD4	biotin	553649	H129.19	Various	BD Biosciences
CD5	biotin	553019	53-7.3	5062988	BD Biosciences
CD8a	biotin	553029	53-6.7	Various	BD Biosciences
CD11b	biotin	553309	M1/70	Various	BD Biosciences
CD45R/B220	biotin	553086	RA3-6B2	8127591	BD Biosciences
Ter119	biotin	553672	TER-119	Various	BD Biosciences
Gr-1/Ly-6G/C	biotin	553125	RB6-8C5	7275907	BD Biosciences
CD45.1	FITC	110706	A20	B202563	Biolegend
CD45.2	Pacific Blue	109820	104	B249623	Biolegend
Ter119	FITC	116206	TER-119	B272256	Biolegend
CD4	PE	130310	H129.19	B200770	Biolegend
CD48	PE	103406	HM48-1	B202873	Biolegend
CD150	PE-Cy7	115914	TC15-12F12.2	B238925	Biolegend
Gr-1/Ly-6G/C	PE-Cy7	108416	RB6-8C5	B209822	Biolegend
CD8a	APC	100712	53-6.7	B207080	Biolegend
CD8a	PE	100708	53-6.7	B223225	Biolegend
CD11b	Pacific Blue	101224	M1/70	B196387	Biolegend
CD11b	PE	101208	M1/70	B228654	Biolegend
CD11b	APC	101212	M1/70	B221810	Biolegend
CD117/c-Kit	APC	105812	2B8	B249344	Biolegend
CD117/c-Kit	BV-510	135119	ACK2	B209927	Biolegend
Sca-1/Ly-6A/E	FITC	122506	E13-161.7	B163258	Biolegend
Sca-1/Ly-6A/E	PE-Cy7	122514	E13-161.7	B194434	Biolegend
Sca-1/Ly-6A/E	Pacific Blue	122520	E13-161.7	B174209	Biolegend
CD19	APC-Cy7	115530	6D5		Biolegend
CD16/CD32	APC-Cy7	101328	93	B232340	Biolegend
CD71	PE	113808	R17217	B194428	Biolegend
CD127	BV-421	135023	A7R34	B241249	Biolegend
CD34	FITC	553733	RAM34	7341852	BD Biosciences
CD135	PE	553842	A2F10.1	8123884	BD Biosciences
CD41	APC	133914	MWReg30	B203704	Biolegend
CD105	PE	120408	MJ7/18	B169023	Biolegend
Streptavidin	PerCP	405213	–	B214631	Biolegend